ChemMedChem

Chemistry Europe
European Chemical Societies Publishing

Accepted Article

Title: Hydrogen Peroxide Inducible Acid-Activatable Prodrug for Targeted Cancer Treatment

Authors: Jun Liu, Jinhua Wang, Shuang Si, Jinyi Xu, and Peng Xue

To be cited as: *ChemMedChem* 10.1002/cmdc.202100354

Link to VoR: https://doi.org/10.1002/cmdc.202100354

WILEY-VCH

10.1002/cmdc.202100354

WILEY-VCH

RESEARCH ARTICLE

Hydrogen Peroxide Inducible Acid-Activatable Prodrug for Targeted Cancer Treatment

Jun Liu*, Jinhua Wang, Shuang Si, Jinyi Xu, and Peng Xue

J, Liu, J, Wang, S, Si, J, Xu, P, Xue
College of Chemistry and Chemical Engineering
Hexi University
Zhangye City 734000, Gansu Province, P. R. China
E-mail: liujun3622849@163.com

Abstract: In view of some of the potentially most useful boronic acids are inherently unstable in the blood plasma and poor selective retention in tumours, 2-heterocyclic N-methylimino diacetic acid (MIDA) boronates provide a safe and spacious harbor for the prodrug conjugates with highly effective and stable platform. We herein proposed that N-methyliminodiacetic acid (MIDA) boronates in concurrent with naphthalene-based fluorophore by virtue of their remarkable capacity and uniform benchtop stability for tumor diagnosis. The shielding group was found to be effective in treating the stability at physiological pH 7.4 but released rapidly to the acidic microenvironment of the tumor. This approach was significantly enhanced drug release efficiency and exhibited fewer side effects, thus indicating its great potential for precision therapeutics.

Introduction

The principle goal of tumor targeting capability is crucial for the accurate diagnosis of tumors. Therefore, improving the therapeutic efficacy of the acidic tumor microenvironment is required before starting therapy.[1-5] The formidable challenge for tumor therapy is how to achieve enhanced permeability and improve the drug therapeutic efficacy with minimum systemic toxicity due to the non specific distribution of small molecular drugs in vivo. However, the severe side effects of many drugs, including systemic instability, poor bioavailability, rapid blood/renal clearance, lack of cancer specificity, and uncontrollable drug release, have impeded the efficient internalization and caused premature drug release in the blood circulation.[6-8] There is an urgent need to inspire the development of fluorescence systems to establish stable, efficient, and multifunction platform for drug delivery in the cancer cells.

Evidence suggests that the aberrant production of H_2O_2 can be a therapeutic advantage, because it is an important regulator of signal transduction.[9-13] The aryl boronic acids and their esters group (deprotection) as species are well-known to be cleaved by H_2O_2.[14-17] This reactivity provides a chem-specific, biologically compatible reaction method for detecting endogenous H_2O_2 production. However, liberation of the boronic acid groups is usually hampered by high toxicity and low cellular uptake, specifically, boronic acids are notoriously unstable, which precludes therapeutic efficacy of heterogeneous tumor environments.[18-21] To circumvent these limitations, we herein report that 2-heterocyclic N-methylimino diacetic acid (MIDA) boronates in concurrent with naphthalene-based fluorophore by virtue of their remarkable capacity and uniform benchtop stability for tumor diagnosis.[22-25] In contrast to other boronates or esters, the effects of manipulating MIDA hydrolysis, which has enabled these dramatic rate differences to the structure of the organic fragment, since they are stable in the blood plasma. Thus, it is important to achieve controlled shielding of loaded drugs in the biodistribution and blood circulation.

We propose that nitrogen mustard as the encapsulating to create a promising framework for overcoming the stability in the blood circulation. The prodrugs of nitrogen mustard coupled with boronic acid or arylboronate derivatives can be selectively activated by H_2O_2 in tumor sites. After the internalization, the prodrugs (L-M-CPT) would disintegrate and release drug CPT rapidly due to the destruction of MIDA boronates under mildly acidic conditions. Using this approach, the stability and stimulus responsive properties of prodrug as stable surrogates can synergistically achieve effectively prevented premature CPT release and achieved prompt intracellular release during intracellular trafficking (Scheme 1).

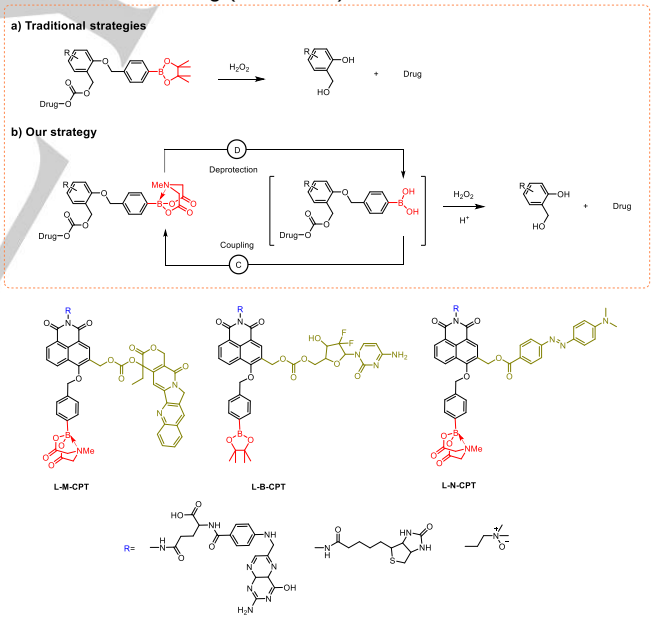

Scheme 1. Schematic representation of the reaction of prodrugs with H_2O_2.

Results and Discussion

To test the proposed the optical sensing behavior of prodrug L-M-CPT toward H_2O_2 by the breakage of the MIDA boronate, the fluorescence properties of probe were carried out under optimum conditions. As shown in Figure 1a, upon addition of H_2O_2 solution, the fluorescence intensities (λ_{ex} =470 nm, λ_{em} = 523 nm) was dependent of different concentrations of L-M-CPT. These

experimental results demonstrated that concentration-dependent enhanced fluorescence (3 μM) could be selected as an appropriate working concentration for monitoring the drug release process with the employed prodrug.

To verify MIDA-induced destruction as illustrated in Scheme 1, fluorescence spectra were used to probe the change of the L-M-CPT from"caged" to "uncaged" state upon activation with H_2O_2. In these experiments, we investigated the spectral properties of the prodrug at 37 °C in phosphate buffer (pH 7.4, 10 mM), as shown in Figure 1a–d. In order to evaluate the ability of MIDA boronates could be cleaved by H_2O_2, the L-M-CPT solution (3 μM) was incubated with H_2O_2 from 0 to 80 eq at 37 °C. After the addition of H_2O_2, the fluorescence intensity around 523 nm exhibits an excellent change with the increasing analyte level, which ascribed to the cleavage of MIDA boronates caused by H_2O_2.

In addition, we also investigated the CPT release behavior under different pH conditions through monitoring the fluorescence changes of 3 μM L-M-CPT. Upon the addition of H_2O_2 (1.0 mM) at pH = 6.0, the CPT was released with the response rate by the fluorescent recovery. However, L-M-CPT exhibits no change by monitoring its fluorescent intensity for at least 1 h at the condition of pH 7.4 (Figure 1c). The above results indicated that L-M-CPT could remain stable in blood circulation while release the active drug quickly in an acidic environment due to the"caged" or "uncaged" state of the boronates. Furthermore, in order to assess the cleavage of MIDA, we evaluated linear relationships of the drug release to the fluorescence intensity at the condition of pH 6.0. The results shown in Figure S13 indicate that the fluorescence signal is linearly correlated with CPT release from the L-M-CPT upon specific activation of H_2O_2.

Subsequently, in order to validate the pH-induced controlled release behavior of L-M-CPT, in vitro drug release profile was further investigated in PBS solutions at 37 °C with different pH values, i.e. pH 6.0 and 7.4 respectively. As displayed in Figure 1d, approximately 90% of CPT has been released from L-M-CPT after being incubated at pH 6.0 for 40 min, whereas only 17.5% of the drug was detected at the condition of pH 7.4. From this point of view, L-M-CPT can maintain its integrity under neutral physiological conditions (blood circulation environment) while specifically trigger rapid release under acidic conditions (tumor environment). In addition, the limit of detection (LOD) was calculated to be 30 nM (S/N=3, Figure S13), indicating the MIDA boronates of the prodrug can be effectively cleaved by H_2O_2. As a control, we also tested the selectivity of L-M-CPT toward H_2O_2 upon incubation with the interfering substances, including metal ions, ROS and RNS. As depicted in Figure S14, S15, the fluorescence response of L-M-CPT showed only neglectable increases after incubation with other biological biomarkers. The above results indicated that L-M-CPT could deliver chemotherapeutics under hydrogen peroxide situation, suggesting that theranostic agent with high selectivity over potential interference to detect H_2O_2 quantitatively.

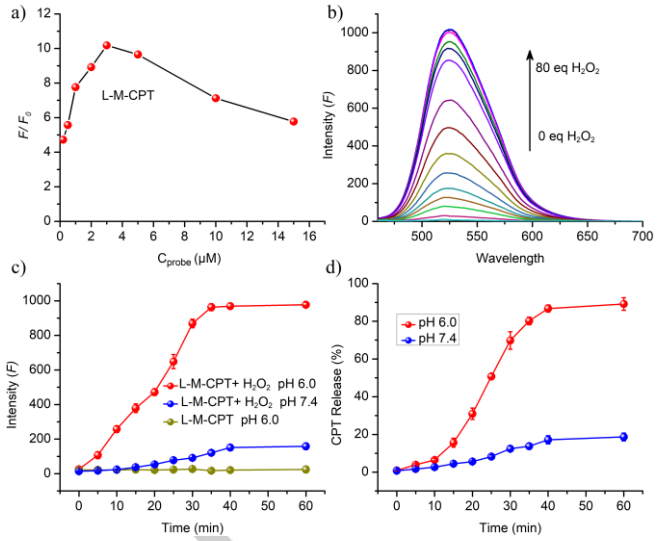

Figure 1. a) Effect of probe concentration (H_2O_2 concentration: 240 μM) in PBS (pH=6.0). b) The fluorescence emission spectra of L-M-CPT (3 μM) in the presence of different concentrations of H_2O_2 at pH 6.0 (PBS). λ_{ex}=470 nm. c) Fluorescence intensity changes of L-M-CPT exposed at pH 7.4 or 6.0 for different time periods. d) In vitro release profiles of CPT from prodrug in PBS under different pH conditions. Error bars were calculated from three independent experiments. Error bars represent ± SD (n = 3).

Subsequently, the H_2O_2-induced release of CPT was also confirmed as monitored by ESI-MS analysis. From the mass spectra, we observed molecular peaks corresponding to CPT ([M+ H] = 349.52) and residue ([M + H] = 684.3) as shown in Figure S11. This is taken as evidence that the hydrolysis of MIDA boronate can release active drug moiety present in L-M-CPT was cleaved by H_2O_2. The above investigations suggest that the MIDA boronate as an outstanding platform by virtue of the uniform benchtop stability for in situ release of the corresponding unstable boronic acids. The sensing mechanism of the MIDA boronate ligand containing L-M-CPT responding to H_2O_2/ H+ was summarized and displayed in Scheme 2.

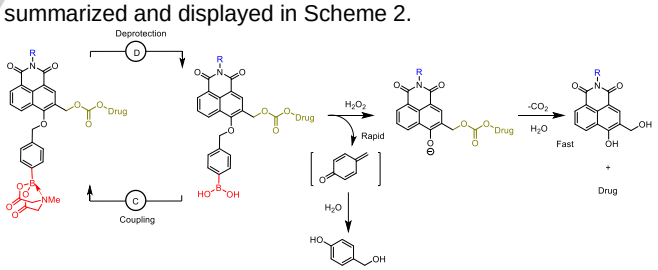

Scheme 2. Proposed drug release mechanism of the reaction of prodrugs with H_2O_2 at the tumor site.

To more precisely demonstrate the drug release process in cancer cells, probes L-B-CPT and L-M-CPT were separately incubated with HeLa cells and B16F10 cells. Figure 2 shows the subcellular location of L-M-CPT and L-B-CPT with that of lysosome indicator (Lyso-Tracker Deep Red) to examine the feasibility of prodrug using folate receptor-enriched tumor cells at 37 °C. After 2.5 h of incubation, the staining of the green fluorescence translocation to the lysosomes shown colocalization with the red fluorescence of the labeled lysosomes with Pearson's correlation coefficient of 0.94, which indicated that drug release of L-M-CPT by H_2O_2 as a result of the acidic microenvironment. The acid-dependent CPT release sustained manner was attributed to the acid-labile MIDA boronate ligand of drug delivery system in

real time. This behavior stands in marked contrast to what is seen in the case of L-B-CPT and is thus consistent with the proposed the instability in the blood circulation.

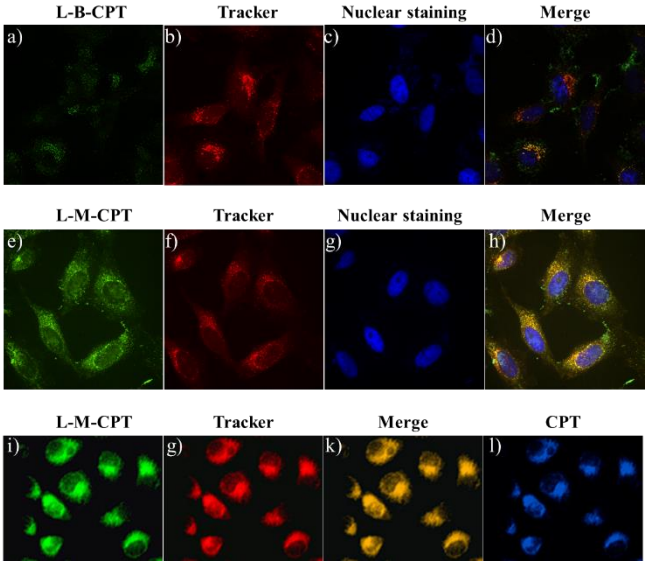

Figure 2. The intracellular trafficking of L-B-CPT (1.0 μM) and L-M-CPT (1.0 μM) by using Lyso-Tracker (colocalization Pearson correlation coefficients, L-M-CPT: 0.94) in HeLa cells at 37 °C (λ_{ex} = 488 nm, λ_{em} = 520–560 nm). The intracellular trafficking of L-M-CPT (1.0 μM) in B16F10 cells at 37 °C.

Encouraged by the intracellular drug release behavior of L-M-CPT used as drug carrier, the cell cytotoxicity of L-M-CPT was investigated quantitatively via an MTT colorimetric assay. As presented in Figure 3, both free CPT, L-B-CPT and L-M-CPT were incubated with HeLa cells show dose-dependent cytotoxicity at pH 7.4 and pH 6.0. With increased concentration of CPT, The CPT-loaded L-M-CPT exhibited the highest cytotoxicity (IC_{50}, 1.21 μg/mL) against HeLa cells at pH 6.0, which was ascribed to the receptor mediated endocytosis and drug released with the protecting MIDA boronate was removed in acidic environments. It also can be observed that the CPT exhibited higher cytotoxicity than prodrug due to the L-M-CPT has markedly reduced cellular uptake as compared with free CPT, consistent with a previous report. Overall, the prodrug exhibited significant anticancer efficacy to cancer cells.

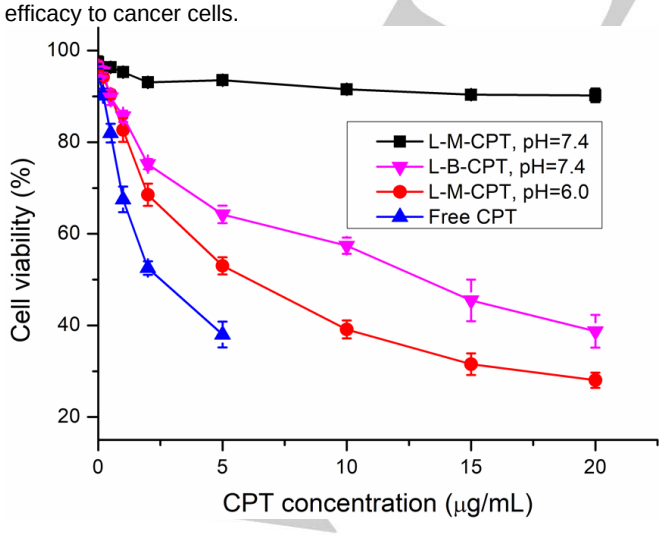

Figure 3. In vitro cell viability assay of L-M-CPT in HeLa cells at pH 7.4 and 6.0 for 48 h. Each error bar represents the standard deviation of 3 replicates.

To demonstrate the biodistribution and tumor accumulation behavior of the drug carriers, the mice were administered intravenously with the L-M-CPT. As shown in Figure 4, the prodrug exhibited strong fluorescence in tumor in the first hour, revealing rapid distribution of the L-M-CPT via the blood circulation and significant drug release by H_2O_2 at the tumor site in vivo. To clearly ascertain the tissue distribution of L-M-CPT in mice, the internal organs after anatomy, including heart, liver, spleen, lung, kidney and tumor, were resected and imaged in vivo after intravenous administration. Analysis of organ distributions showed low fluorescent intensities in the liver, lung, and kidney. In contrast, the tumor bestowed the strongest fluorescence, indicating that majority of prodrug could successfully accumulated and the CPT released by plentiful H_2O_2 at the tumor site. More importantly, there were no selective accumulation in the heart, indicating that the prodrug could effectively avoid the drug cardiotoxicity. Together, the results collectively support the active MIDA boronate ligands of L-M-CPT as vehicles exhibited prominent tumor targeting capacity in tumor sites via receptor-mediated endocytosis.

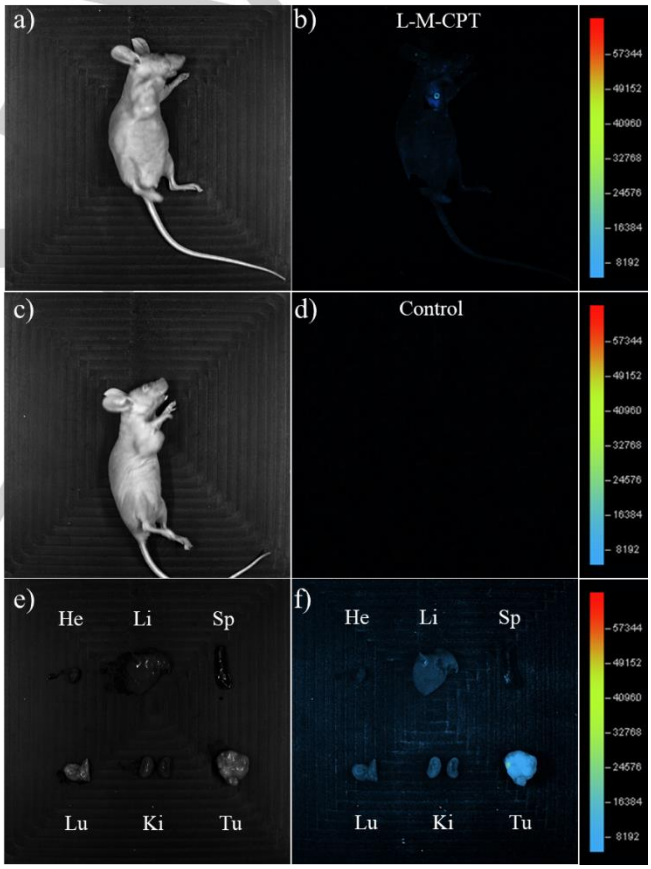

Figure 4. White light (a, c) and fluorescence (b, d) images of BALB/c-nude tumor bearing mice injected with L-M-CPT. Dissected tumor region, major organs (e) and the corresponding fluorescent images (f) form tumor-bearing mice after injection with L-M-CPT, He = heart, Li = liver, Sp = spleen, Lu = lung, Ki = kidney, Tu = tumor.

Enhanced tumor-specific accumulation of prodrug in vivo offers opportunities to evaluate the antitumor effect, as observed by measuring tumor size and subcutaneous inoculation into HeLa-inoculated xenograft murine model every three days. Mice were injected with 3 mg/kg of CPT and CPT-loaded prodrug at days 3, 6, 9, 12, 15, 18 and 21. The tumor xenograft volume after

administration of the prodrug, PBS and free CPT are shown in Figure 5. Among the three groups, tumors treated with the L-M-CPT demonstrated significant growth inhibition compared with control group (PBS and free CPT). After 21 days, significant reductions in tumor volume were monitored, indicates its target specificity. In contrast, the tumors of the mice injected with free CPT and PBS grew rapidly over time. Within the same time frame, 29.7-fold increase for free CPT and 46.6-fold increase for PBS. The results revealed that folated-prodrug could enhance the antitumor efficacy and low side effects in the acidic tumor microenvironment, supporting the remarkable potential drug release utility for effective diagnosis and therapy of cancer.

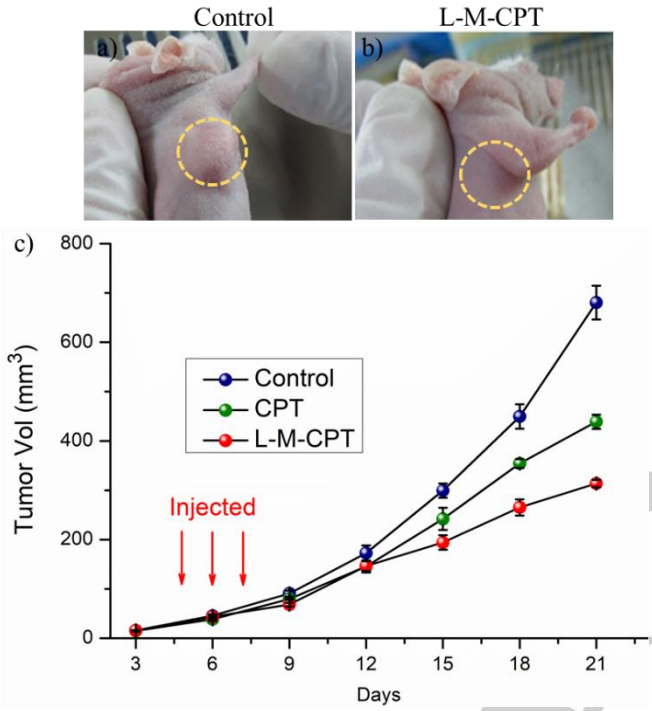

Figure 5. In vivo chemotherapeutic effects of L-M-CPT in a xenograft mouse model. (a) (b) In vivo imaging of solid tumors in HeLa cell-inoculated xenograft mice. Probe L-M-CPT (3 mg/kg), Control (PBS) and CPT (3 mg/kg)-induced regression of tumors. (c) L-M-CPT was injected into the tail vein two times per week for 3 weeks. Tumor size gradually decreased upon treatment with L-M-CPT. Results are representative of three independent experiments (n = 3). Error bars are ±SD.

Conclusion

In summary, we develop a new functionalized theranostic agent, L-M-CPT, which contains N-methyl iminod iacetic acid (MIDA) boronates represent the prodrug can balance intracellular release of anticancer drugs and extracellular shield of the circulation of blood. The therapeutic efficacy and specificity of the prodrug can be enhanced by combining benchtop stability and versatile approach for improved cancer therapy. It was found that the L-M-CPT can effectively internalize into tumor cells and release the drug CPT upon reaction with cellular H_2O_2. These findings clearly indicate that L-M-CPT is effectively internalized by receptor-mediated endocytosis within biotin receptor-enrich cells. This approach can provide both therapeutic effect evaluation and drug delivery imaging information, ensuring improved understanding of cellular uptake and release mechanisms of drugs. Therefore, our probe, described above, could provide a promising framework for overcoming the stability in the blood circulation and achieving drug release in acidic tumor environments.

Acknowledgements

We would like to acknowledge the financial support of the Young Science and Technology Plan Project of Gansu Province (20JR5RA193), and the General Program of the Key Laboratory of Hexi Corridor Resources Utilization of Gansu Universities (XZ2003), and the PhD Start-up Foundation of Hexi University of China (KYQD2020010).

Keywords: hydrogen peroxide • MIDA • prodrug • cancer treatment • tumor environments

[1] M. T. Manzari, Y. Shamay, H. Kiguchi, N. Rosen, M. Scaltriti, D. A. Heller, *Nat. Rev. Mater*. **2021**, *6*, 351-370.
[2] M. Izci, C. Maksoudian, B. B. Manshian, S. J. Soenen, *Chem Rev*. **2021**, *121*, 1746-1803.
[3] J. L. Kolanowski, F. Liu, E. J. New, *Chem. Soc. Rev*. **2018**, *47*, 195-208.
[4] H. M. Hollandsworth, M. A. Turner, R. M. Hoffman, M. Bouvet, *Surg Oncol*. **2021**, 36, 84-90.
[5] A. Haque, M. S. H. Faizi, J. A. Rather, M. S. Khan, *Bioorg Med Chem*. **2017**, *25*, 2017-2034.
[6] J. Xing, Q. Gong, Q. U. Akakuru, C. Liu, R. Zou, A. Wu, *Nanoscale*. **2020**, *12*, 24311-24330.
[7] J. Gregory, M. D. Burgio, G. Corrias, V. Vilgrain, M. Ronot, *JHEP Reports*. **2017**, *2*, 100100-100112.
[8] P. Wu, X. Wang, Z. Wang, W. Ma, J. Guo, J. Chen, Z. Yu, J. Li, D. Zhou, *ACS Appl. Mater. Interfaces*. **2019**, *11*, 18691-18700.
[9] J. Q. Wang, Y. Q. Zhang, E. Archibong, F. S. Ligler, Z. Gu, *Adv. Biosys*. **2017**, *1*, 1700084-1700099.
[10] Z. Wu, M. M. Liu, Z. C. Liu, Y. Tian, *J. Am. Chem. Soc*. **2020**, *142*, 7532-7541.
[11] Y. M. Lee, W. F. He, Y. C. Liou, *Cell Death Dis*. **2021**, *12*, 58-71.
[12] Y. A. Bogdanova, C. Schultz, V. V. Belousov, *Curr Protoc Chem Biol*. **2017**, *9*, 117-127.
[13] S. García-Santamarina, S. Boronat, E. Hidalgo, *Biochem*. **2014**, *53*, 2560-2580.
[14] Y. Liao, L. P. Xu, S. Y. Ou, H. Edwards, D. Luedtke, Y. Ge, Z. H. Qin, *ACS Med. Chem. Lett*. **2018**, *9*, 635-640.
[15] J. Liu, C. Cao, *ACS Omega*. **2020**, *5*, 22157-22162.
[16] E. W. Miller, O. Tulyathan, E. Y. Isacoff, C. J. Chang, *Nat Chem Biol*. **2007**, *3*, 263-267.
[17] B. C. Dickinson, C. Huynh, C. J. Chang, *J. Am. Chem. Soc.* **2010**, *132*, 5906-5915.
[18] Y. Lu, B. Peng, X. Qiu, X. Li, Z. Li, D. Zhang, W. Ji, B. Fang, Q. Wu, C. Zhang, L. Li, W. Huang, *Mater. Adv*. **2020**, *1*, 1448-1454.
[19] X. Song, S. Bai, N. He, R. Wang, Y. Xing, C. Lv, F. Yu, *ACS Sens*. **2021**, *6*, 1228-1239.
[20] J. Liu, S. Zhou, J. Ren, C. Wu, Y. Zhao, *Analyst*. **2017**, *142*, 4522-4528.
[21] Y. Huang, W. Zhang, Y. Xu, S. Zhu, Y. Wu, T. Chen, Y. Xiao, W. Lu, X. Zhang, J. Yu. *Int J Pharm*. **2020**, *580*, 119250-119261.
[22] A. J. J. Lennox, G. C. Lloyd-Jones, *Chem. Soc. Rev*. **2014**, *43*, 412-443.
[23] Y. Zeng, X. Liu, D. Tan, W. Fan, Y. Li, Y. Guo, H. Wang, *Chem. Commun*. **2020**, *56*, 4332-4335.
[24] A. M. Kelly, P. Chen, J. Klubnick, D. J. Blair, M. D. Burke, *Org Lett*. **2020**, *22*, 9408-9414.
[25] A. D. Steinkamp, S. Wiezorek, F. Brosge, C. Bolm, *Org Lett*. **2016**, *18*, 5348-5351.

Entry for the Table of Contents

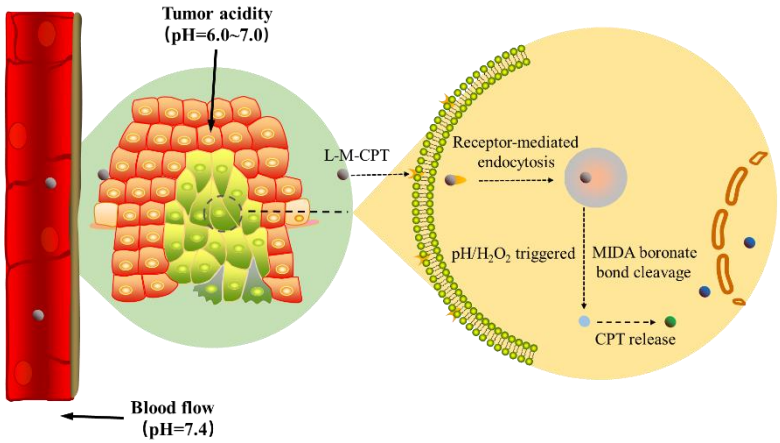

To achieve controlled shielding of loaded drugs in the biodistribution and blood circulation, we propose that nitrogen mustard as the encapsulating to create a promising framework for overcoming the stability in the blood circulation. The prodrugs of nitrogen mustard coupled with boronic acid or arylboronate derivatives can be selectively activated by H_2O_2 in tumor sites. Using this approach, the stability and stimulus responsive properties of prodrug as stable surrogates can synergistically achieve effectively prevented premature CPT release and achieved prompt intracellular release during intracellular trafficking. Therefore, the probe, could provide a promising framework for overcoming the stability in the blood circulation and achieving drug release in acidic tumor environments.